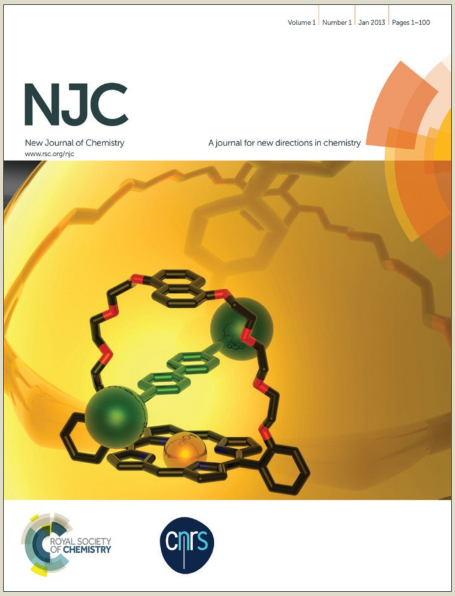
Volume 1 | Number 1 | Jan 2013 | Pages 1–100
NJC
New Journal of Chemistry
www.rsc.org/njc
A journal for new directions in chemistry
ROYAL SOCIETY OF CHEMISTRY
cnrs

New Journal of Chemistry

ARTICLE

On the nature of the phase “η-TiO_2”

Inga Vasilyeva[a], Galina Kuz’micheva[b], Alena Pochtar[c], Asiya Gainanova[b†], Olesya Timaeva[b], Andrey Dorokhov[b] and Vadim Podbel’skiy[d]

Received 00th January 20xx,
Accepted 00th January 20xx

DOI: 10.1039/x0xx00000x

www.rsc.org/

Conditions for the sulfate method of the synthesis of a metastable modification, which has been previously described as “η-TiO_2” (Dadachov M., 2006), were found and the stability region of this phase in the hydrolysis temperature–hydrolysis duration coordinates was determined. Investigation by a complex of methods (X-ray powder diffraction, differential dissolution method, thermogravimetry, IR spectroscopy, Raman spectroscopy) showed that the η-phase is not a polymorph of TiO_2 but is a pseudo-polymorph of titanium dioxide hydrate. It was demonstrated that nanoparticles of the low-temperature η-phase consist of the [$TiO_{2-x}\cdot mH_2O$] core, the structure of which can be described as a superstructure in relation to anatase, and an amorphous shell containing TiO_{2-x} (trace amount), OH, HSO_4 and water. The average crystallite size depends on the ratio of the constituents.

Introduction

Polymorphism is the ability of compounds to exist in more than one forms having different crystal structures and properties, the chemical composition being the same (in some cases, in the homogeneity region), depending on the external conditions. The latter include the temperature, pressure, different types of fields (electrical, magnetic, *etc.*), the mode of treatment of materials (heat, microwave, ultrasound, *etc.*), the duration of treatment, and so on, *i.e.*, the thermodynamic and kinetic factors. Therefore, the *polymorphism* is one of the key properties of compounds than enables their structures to be adapted to varying external conditions.

Theoretical and experimental studies of the thermodynamics of small particles showed that the particle size is an active variable responsible, together with other thermodynamic variables, for the state of the system. The changes in the particle size are associated with some thermodynamic properties of nanoparticles (the concentration of vacancies in nanoparticles increases with a decrease in their size, which is accompanied by a reduction of the polymorphic transition temperature and the unit cell parameters and an increase in the compressibility and solubility) and physicochemical properties (stability, heat capacity, melting point, electric and magnetic characteristics, reactivity, *etc.*). The particle size can be considered as a specific equivalent of the temperature. In this case, the Gibbs potential will differ from the standard parameters of the bulk phase. The character of the dependence G=f(L) (G is the Gibbs free energy and L is the crystallite size) with a minimum at L_{crys} implies that the formation of crystallites in the range $L<L_{crys}$ becomes thermodynamically unfavorable [1]. Therefore, it can be suggested that energy minima (both global and local) can appear at different values of L for different nanosized polymorphic modifications as stable and metastable, respectively. In other words, rather large sets of polymorphs or modifications can be obtained by controlling nanostructuring processes. Consequently, physicochemical concepts are supplemented with the terms “size” and “self-organization”.

Currently, titanium(IV) oxides seem to be the most interesting from the theoretical and practical points of view. Twelve polymorphs of titanium dioxide, which were prepared either under ambient conditions or at high temperatures and elevated pressures, were described in the literature. These polymorphs include metastable modifications (for example, anatase β-TiO_2) and stable modifications (for example, rutile), which either have or do not have homogeneity regions and which were synthesized as nanosized (primarily, anatase, brookite, rutile, β-TiO_2) and bulk (all 12 modifications) samples.

Nano-TiO_2 with an anatase structure is more widely used in practice compared to other modifications. Thus, it possesses photocatalytic activity (PCA) in the UV region of the solar spectrum [2-5], has high chemical stability, is inexpensive and non-toxic and, consequently, is a promising compound for the design of solar photoelements [6] and photocatalysts active in the visible region of the spectrum [3, 4, 7, 8].

A new modification of titanium dioxides, called “η-TiO_2“, which has been synthesized relatively recently only as nanosized form [9], largely outperforms anatase in adsorption properties [10]. In [11] this phase was shown to have high PCA at pH > 7, where the reaction rate of the decomposition of organic dyes under UV

---

[a] Institute of Inorganic Chemistry, Siberian Branch of the Russian Academy of Sciences, Novisibirsk, Russia.
[b] Lomonosov State University of Fine Chemical Technologies, Moscow, Russia.
[c] Boreskov Institute of Catalysis, Siberian Branch of the Russian Academy of Sciences, Novisibirsk, Russia.
[d] National Research University "Higher School of Economics", Moscow, Russia
† corresponding author, e-mail address ms.asenka1984@mail.ru

irradiation is an order of magnitude higher than that in the presence of photocatalysts based on other modifications of titanium dioxide (anatase and/or rutile) studied earlier. It was hypothesized [9, 10] that the high reactivity of the surface of samples with the η-phase is due to a larger amount of OH groups on the surface of nanoparticles compared to anatase.

It should be noted that "η-TiO_2" is merely the molecular formula, whereas the structure and the real composition of this phase are unknown. Therefore, it is impossible to assign this phase to polymorphs of titanium dioxide and explain its specific properties. The goal of the present study is to answer these questions.

Experimental

Synthetic procedures

Samples of the η-phase were prepared by the hydrolysis of titanyl sulfate $TiOSO_4 \cdot xH_2SO_4 \cdot yH_2O$ at a constant pH value of the solution (pH~2) and at a constant concentration of the starting reagent (c_0 = 0.65 mol/L). After the completion of the hydrolysis (τ = 5-80 min, t = 50-95°C), the coagulation was performed using a 1.3 mol/L KCl aqueous solution followed by the filtration of the precipitate, washing it with water (until titanium and sulfate ions were not found in the washing waters) and acetone, and drying in an oven for 1 h at 50°C [12, 13].

Methods

X-ray powder diffraction. X-ray powder diffraction data were collected on a HZG-4 diffractometer (Ni filter): CuK_α radiation with a diffracted beam monochromator in the step-scan mode (the count time was 10 s per step, the scan step was 0.02°, the scattering angle range 2θ = 2−50°). The value of *D,* which determines the average size of coherent scattering region (*D*) or crystallite sizes (*L)* (in the case of their equality), was calculated by the Warren formula [14] (without account for possible microstrains) $D = K\lambda/\beta\cos\theta$, where λ = 1.54051 Å is the wavelength, 2θ~25° (*d*~3.5Å; anatase, 101 diffraction reflection) and 2θ~27.5° (*d*~3.25Å; rutile, 110 diffraction reflection), and β-TiO_2 is the broadening of the reflection compared with the instrumental width ($\beta=[(F_{WHM})_{exp}^2-(F_{WHM})_R^2]^{1/2}$, where $(F_{WHM})_{exp}$ and $(F_{WHM})_R$ are the peak widths at half maximum for titanium dioxide and the reference α-Al_2O_3, respectively); the coefficient *K* (Scherrer coefficient, the shape factor of crystallites) was taken equal to 0.9. The standard deviation was ±5%. The percentage of anatase in samples with rutile was calculated by the equation $x_R,\% = [1+0.65(I_A/I_R)]^{-1}$, $x_A,\% = 100-x_R$, where I_A and I_R are the integrated intensities of anatase for the 101 diffraction reflection and of rutile for the 110 reflection, respectively.

In order to performed the theoretical analysis of powder diffraction patterns of two-phase mixtures and determine the percentage of anatase and "η-TiO_2" in samples, we wrote the supplemental program Technol-1 [15], which can be used to obtain a linear combination of the initial diffraction patterns of single-phase samples. The program was written in C# oriented to the Net Framework platform (versions 3.5 and higher). Text files containing numerical data from powder diffraction patters serve as the starting data. When analyzing the diffraction patterns and their linear combinations, the maximum intensity at a particular value of the variable xi (2θ°) was estimated for each diffraction reflection taking into account the background level.

Stoichiographic differential dissolution method. Basic principles and apparatus for the method of differential dissolution (DD) were described in detail in [16]. The method serves for the phase analysis and is used to identify phases from their composition regardless of the degree of crystallinity assuming that, during the dissolution of the individual phase, the atomic ratio of the constituent elements is the same as that in the solid state. The dissolution is performed in a solvent flow with a composition, which varies according to a preset program and is supplied to the reactor containing a sample using peristaltic pumps at intervals of 3-5 s. The resulting solution is directed to a detector to determine the content of all elements that were transferred to a solution from the solid sample. After the complete dissolution of the sample, 300-650 aliquots of the solution are usually analyzed. The amounts of elements, which were transferred to the solution, are determined regardless of their chemical form and oxidation state, by inductively coupled plasma atomic emission spectroscopy (ICP AES). In the presence of several phases in the solid sample, conditions are created for the sequential dissolution of phases by using the dynamic mode of dissolution and a solvent with a continuously increasing chemical potential. During the period of complete dissolution of the solid sample, dissolution kinetic curves for all constituent elements are recorded.

Solvents, in which phases of different nature can be successively dissolved, were used for the DD analysis of samples. Since hydrated forms of Ti^{4+} are easily dissolved in an aqueous or weak nitric acid medium, whereas titanium dioxide can be dissolved only in strong hydrofluoric acid, the composition of the solvent was gradually changed from water at 25°C to HNO_3 (pH = 2) at 25-40°C, 3N HNO_3 at 40-70°C, and finally 4N HF at 80°C. In the case of dissolution of titanium compounds with different compositions, an ICP AES detector was adjusted to the determination of titanium, sulfur, and potassium contents because the samples were synthesized in the presence of sulfuric acid, which is known [17-19] to act as a good coordinating ligand, and KCl was added as a coagulant. Preliminary experiments showed that the potassium content was low (<2%) and this element was randomly captured by the bulk of the product that precipitated. This is evidence that potassium chloride is not involved in the formation of coagulation phases.

Thermoanalytical DTA (differential thermal analysis) coupled with TGA (thermogravimetric analysis). Heating curves were recorded on a DTG6OH instrument in an air flow at a heating rate of 10°C/min in the temperature range from 25 to 1500°C; the weight of the sample was 20 mg.

Vibrational IR (infrared)) spectroscopy. Raman spectroscopy. The IR spectra were recorded on a VERTEX 80 Fourier-transform infrared spectrometer and an UV-3101 PC UV-VIS-NIR spectrometer (Shimadzu) as KBr pellets, Nujol mulls or in fluorinated oil. Raman spectra were measured on a SPEX 1877 Triple spectrometer with excitation at 488 nm by an argon laser.

Results and discussion

In present paper the studied samples were prepared by the hydrolysis of titanyl sulfate $TiOSO_4 \cdot xH_2SO_4 \cdot yH_2O$ at different duration (τ = 5-80 min) and temperature (t = 50-95°C). As it was found earlier [9, 20], the η-phase is characterized by a strong diffraction reflection with an interplanar spacing in the range d ~ 17–21 Å and a less intense reflection with d ~ 2.7–2.9 Å, the other reflections (d ~ 3.5, ~1.9, ~1.7, ~1.5 Å) being the same as those of TiO_2 with an anatase structure (sp. gr. $I4_1/amd$, a ~ 3.785 Å, c ~ 9.50 Å; JCPDS 89-4921). It was impossible to determine the crystal structure of this compound because the η-phase is characterized by very small sizes of coherent scattering regions (D~30-50 Å) related to crystallite sizes [9], as well as by a limited number of reflections. It cannot be ruled out [12, 21-23] that the structure of the η-phase can be considered as a superstructure with respect to the anatase structure with the unit cell parameters a~a_0, c~$2c_0$ (a_0 and c_0 are the unit cell parameters of anatase). It should be noted that the indexing of a small number of diffraction reflections of "η-TiO_2" indicates the Bravais lattice P and limits the possible tetragonal space groups to $P4/mmm$ ($P\bar{4}2m$, $P\bar{4}m2$; $P4mm$, $P422$), $P\bar{4}2_1m$; $P42_12$ [12]. It was noted [9] that the absence of the diffraction reflection with d~2.4 Å and the asymmetry of the peak with d~3.5 Å toward smaller angles attest to the single-phase state of the sample (η-phase), whereas the asymmetry of the peak with d~3.5 Å toward higher angles, along with the presence of the reflection with d~2.4 Å, are indicative of the two-phase state of the sample (anatase + η-phase). The average crystallite sizes of the η-phase (L~55–90 Å) determined by transmission electron microscopy [20, 21] are inconsistent with the average sizes of coherent scattering regions (D~30–50 Å) [12, 20-23]. Therefore, the defect structure of the sample cannot be ruled out.

The detailed study of the effect of the conditions for the preparation of samples (the hydrolysis temperature and duration, the presence or the absence of the coagulant KCl at a constant concentration of the precursor c_0 = 0.65 mol/L) on the formation of nano-anatase and the η-phase revealed two parameters – the hydrolysis temperature (t) and the hydrolysis duration (τ) – that play a key role in the formation of these phases. Based on the results of the synthesis in the t range from 50 to 95°C and the τ range from 5 to 80 min and the characterization of 40 samples of titanium dioxide by X-ray powder diffraction, the regions of the existence of nano-anatase, η-TiO_2, and their mixture were found, as shown in Fig. 1.

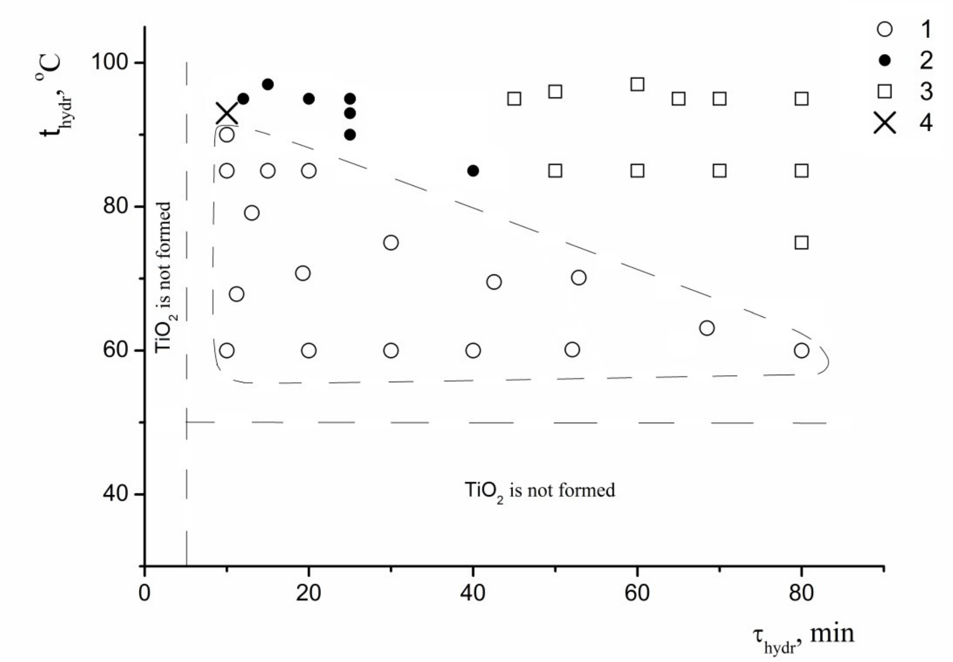

Figure 1. Regions of the existence of anatase and the η-phase in the hydrolysis temperature (t_{hydr}) – hydrolysis duration (τ_{hydr}) coordinates: 1 – η-phase; 2 – anatase + η-phase; 3 – anatase; 4 – sample I.

For subsequent detailed study, we chose sample I (it is marked with an asterisk in Fig. 1) from the two-phase region. Figure 2a shows the powder diffraction pattern of this sample with diffraction reflections at 2θ~5° (d~18 Å), ~25° (d~3.55 Å), and ~33° (*d*~2.7 Å), a very diffuse reflection at 2θ~38° (*d*~2.4 Å), and a reflection at ~48° (*d*~1.9 Å).

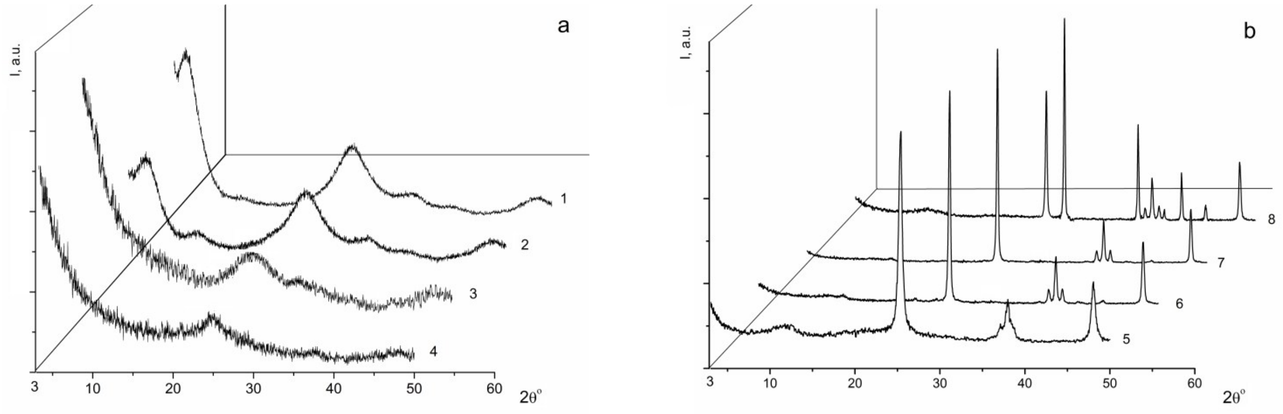

Figure 2. X-ray powder diffraction patterns: *a*, the initial sample I (1), the theoretical powder diffraction pattern of a mixture of anatase (20%) and η-TiO_2 (80%) (2) annealed for 1 h at 150°C (3) and 300°C (4); *b*, of sample I annealed at 650°C (5), 700°C (6), 800°C (7), and 950°C (8).

According to the X-ray diffraction data for sample I (Fig. 2a) and based on a comparison of the diffraction pattern of this sample with the theoretical diffraction pattern (Figs. 2a, 2), this sample is composed of a mixture of anatase and the η-phase in amounts of 20% and 80%, respectively. The additional diffraction peak at 2θ~12° can be assigned either to an amorphous phase of the composition $H_2Ti_xO_{2x+1}$ with *x* = 6, 7 or to amorphous hydrated titanium dioxide $Ti^{4+}O_{2-y/2}(OH)_{1-y}\cdot nH_2O$ (*n*~1) [9]. The average sizes of coherent scattering regions (*D* = 48(2) Å) are indicative of a large fraction of the amorphous component, which is characteristic of all samples with the η-phase [12, 20-23].

Sample I was annealed in air for 1 h at different temperatures: 150ºC (sample I-150, Fig. 2*a,* 3), 300ºC (sample I-300, Fig. 2*a,* 4), 650°C (sample I-650, Fig. 2*b,* 5), 700ºC (sample I-700, Fig. 2*b,* 6), 800°C (sample I-800, Fig. 2*b,* 7), and 950ºC (sample I-950, Fig. 2*b,* 8). As can be seen in Fig. 2, the fraction of the amorphous component in samples I-150 and I-300 is larger, being most pronounced in I-150. It should be noted that the peak at 2θ~5° (*d*~18 Å) is absent in the X-ray diffraction pattern of sample I-150, although the diffuse peak at 2θ~33° (*d*~2.7 Å) characteristic of the η-phase is still observed. The latter peak is absent in the diffraction pattern of sample I-300 (Fig. 2*a,* 4). Samples I-650, I-700, and I-800 contain nano-anatase with crystallite sizes *D* = 195(7) Å, *D* = 270(10) Å, and *D* = 330(15) Å. Sample I-950 consists of two phases and contains 63% of rutile (*D* = 460(20) Å) and 37% of anatase (*D* = 445(20) Å). Therefore, the η-phase can be assigned to the low-temperature metastable form of titanium(IV) oxide.

It is known that the formation of single-phase anhydrous TiO_2 with an anatase structure in sulfuric acid solutions of titanyl sulfate occurs only in the case of the complete hydrolysis. If the hydrolysis is not complete (limited duration of hydrolysis), solid products of varying and unpredictable composition are obtained depending on the degree of hydrolysis and polycondensation of the chemical forms of titanium existing in solution [17, 24-26]. We chose the composition of the ultimate polymer $\{(TiO)_{10}(HSO_4)(OH)_{19}\}_x$, which was deduced taking into account coordinative and chemical saturation and which was further confirmed by direct chemical analysis [17], as the model of the expected partial hydrolysis product obtained under the conditions of the synthesis of sample I. This formula bears anatase structural information at the molecular level, where the $(TiO^{2+})_n$ fragment reflects the planar structure of the -O-Ti-O-Ti- chains in anatase and HSO_4 and OH groups coordinated to titanium [17].

The overall composition of sample I was determined by ICP AES after the dissolution of five different weighed samples in hot 4N HF and the adjustment of the detector to the determination of Ti and S. The element contents expressed in the contents of Ti→TiO and S→HSO_4 fragments, respectively, were summarized and subtracted from the weight of the sample. The difference was related to the hydroxyl group content. According to the results of calculations, the overall composition of the sample determined by the DD method is $(Ti^{4+}O)(HSO_4)_{0.38}(OH)_{1.03}$, and the chemical unsaturation attests to the heterogeneity of sample I.

Then we employed the DD method, which makes it possible, by selectively dissolving phases, to determine the spatial variation in the composition as a function of the volume during the dissolution of each phase comprising sample I.

Figure 3a shows kinetic curves for the elements Ti and S that are transferred to a solution at every instant of time during the complete dissolution of 0.80 mg of the starting sample I. The kinetic curves were constructed from the results of analysis of 650 aliquots of the solution.

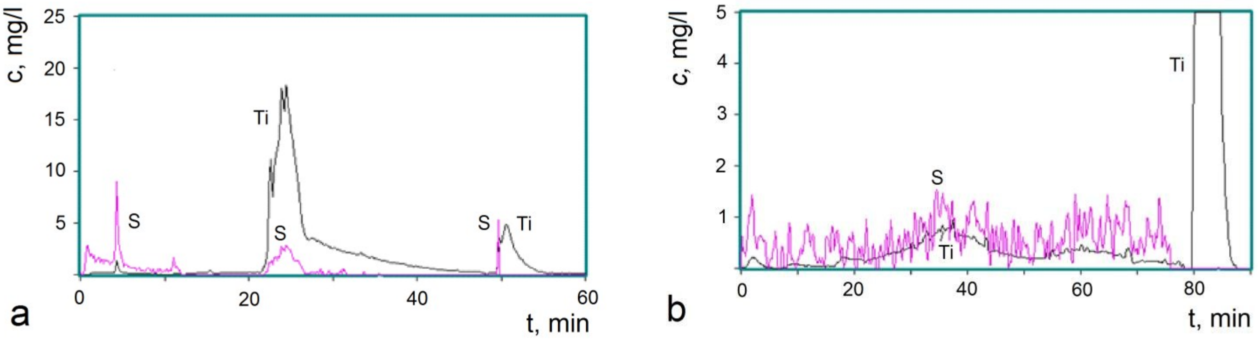

Figure 3. Kinetic curves for the elements Ti and S during the dissolution of sample I (a) and sample I-150 (b):

a. Sample I. The solvent: H_2O up to 10 min; HNO_3, pH=2, at 75°C up to 25 min; 3N HNO_3 at 80°C up to 48 min; 3.8 N HF at 80°C up to 60 min.

b. *Sample I-150.* The solvent: H_2O up to 5 min; HNO_3, pH=2, at 75°C up to 20 min; 3N HNO_3 at 80°C up to 80 min; 3.8 N HF at 80°C up to 90 min.

As can be seen in Fig. 3a, the phases are dissolved successively without overlapping, the dissolution of each next phase starting after the dissolution of the previous one. This is evidence that sample I is composed of three phases, which differ from each other in the chemical potentials of dissolution. The first phase (A) is dissolved in aqueous and weak acid media, during which titanium and sulfur are transferred to the solution. The dissolution of the second phase (B) is a more complicated process: one part (B1) is dissolved in the medium-strength acid HNO_3, during which titanium and sulfur ions are transferred to the solution, whereas another part (B2) is dissolved in 3N HNO_3 at 80ºC and provides only titanium ions to the solution. This character of the dissolution of phases is typical of core−shell nanosized assemblies [27]. In the case under consideration, the phase B2, being a core, has pronounced oxide nature, whereas the shell B1 is composed of titanium(IV) oxide modified by sulfate and hydroxyl groups. The latter are not directly determined by the DD method, but the presence of fluctuations in the dissolution curves is indicative of the partial occupancy of the surface by hydroxyl groups as well. The third phase (C) is dissolved in HF, resulting in the transfer of titanium and sulfur ions to the solution, although in a limited amount. The largest amount of sulfate groups was found in the phase A. The amount of these groups is substantially smaller in the phase B1 and particularly in the phase C. All phases are characterized by an essential difference between the bulk composition of dissolved particles and the composition of the surface modified by sulfate and hydroxyl groups.

The compositions of the phases were determined from the ratio of the averaged molar TiO/HSO_4 fractions, and the content of the phases was expressed as the total weight of titanium and sulfur ions that were transferred to a solution during the single-phase dissolution. These quantitative data are summarized in Table 1 as a balance matrix, which reflects the distribution of the total number of moles of each fragment in the formula $(TiO)(HSO_4)_{0.38}(OH)_{1.03}$ between the three phases.

Table 1. Phase and chemical characteristics of sample I (differential dissolution (DD) method)

Sample / Phases	TiO (mol)	HSO_4 (mol)	TiO/HSO_4 (mol)	Weight fractions %
Sample I	7.28	2.46	1: 0.38	100
Phase A	0.15	1.48	1: 10	2
Phase B (B1+B2) Phase B1 Phase B2	6.12 4.00 2.12	0.92 0.92 -*	1: 0.15 1: 0.25 TiO_x	86 62 24
Phase C	0.94	0.03	1: 0.1	12

* not found.

In order to obtain additional data on the nature of the phases found in sample I, the thermal stability of the latter was studied after storage under different isothermal conditions. The loss of volatile anionic groups was detected and the solid residues were analyzed to determine the overall composition by ICP AES and of the phase composition by the DD method. The kinetic dissolution curves for sample I-150 are shown in Fig. 3b, where 9% of the weight loss leads to a significant change in the phase state of the sample compared to the starting sample I (Fig. 3a). The phase A was depleted in sulfur, the phase B2 disappeared, the composition of the phase B1 changed with simultaneous loss of HSO_4 and OH groups and the reactivity of the latter was reduced, which indicates that the composition acquired oxide nature. This phase is slowly dissolved even in hot 3N HNO_3. After the storage at 300ºC (sample I-300, Fig. 2a, 4) accompanied by 18% weight loss, the phase A disappeared, the phase B1 was also almost completely disappeared, the fraction of the phase C substantially increased, and the amorphization of the product was enhanced. The phase changes in these samples were studied by X-ray powder diffraction and are displayed in Fig. 2. The Raman spectra of the samples presented below confirm this fact.

The nature of the phase B is of most interest. This phase displays the co-dissolution of phases of different composition lying at the basis of sample I. The content of this phase was estimated by the DD method at about 86(2)% (80(2)% according to the X-ray powder diffraction data). The quantitative changes in the phase composition of the starting sample *versus* the temperature of the synthesis are shown in Fig. 4.

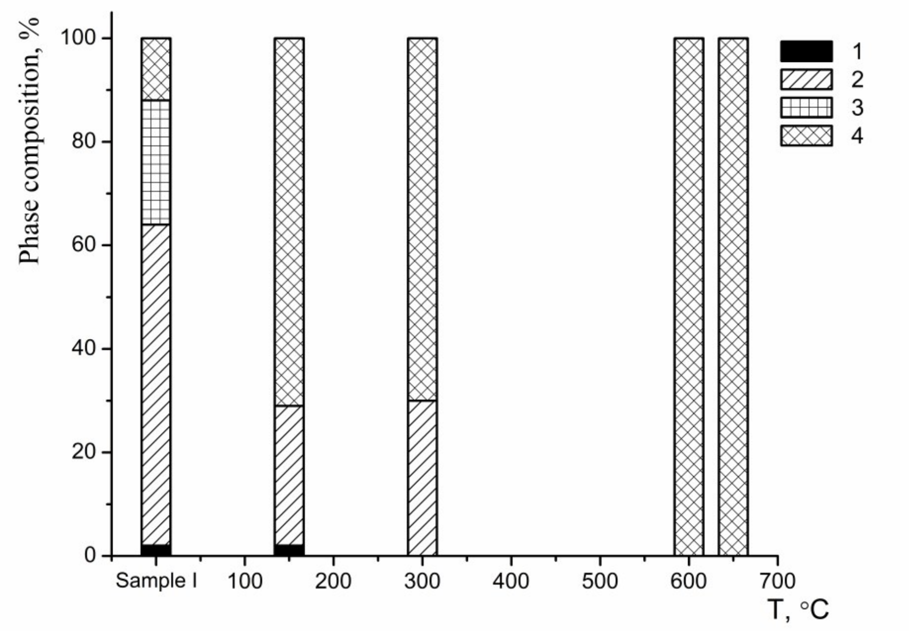

Figure 4. Changes in the phase composition of sample I after the one-hour annealing: 1 – phase A; 2 – phase B1; 3 – phase B2; 4 – phase C.

Therefore, the phase characterization of sample I by the DD method based on the chemical potentials of the solubility of phases as signs of their individuality involves the detection of three phases: the phase A containing a small amount of titanium(IV) oxide (1-2%) and a large amount of sulfate and hydroxyl groups, the phase B (86%), which is the η-phase composed of a core (B2) containing titanium(IV) oxide and a shell (B1) in the form of an intermediate phase of variable structure $(TiO)(HSO_4)_x(OH)_y$ (Fig. 5a), and the phase C with an anatase structure (12%). At a temperature below 600ºC, the latter phase is also most likely composed of a core containing titanium(IV) oxide and a sulfate shell; the size of the latter is much smaller than that of the η-phase (Fig. 5*b*). We attribute this fact to the different dimensionality of the particles of both phases, which is confirmed y the average sizes of *D*: these sizes for the samples with nano-anatase prepared by the sulfate method are substantially larger (*D*~80-90 Å) [21] compared to the samples containing the η-phase (*D*~30-50 Å). It is not improbable that the η-phase is partially transformed into nano-anatase accompanied by the formation of a defect structure (Fig. 5*c*) with $D \neq L$, which is confirmed by the results of earlier studies [20, 21].

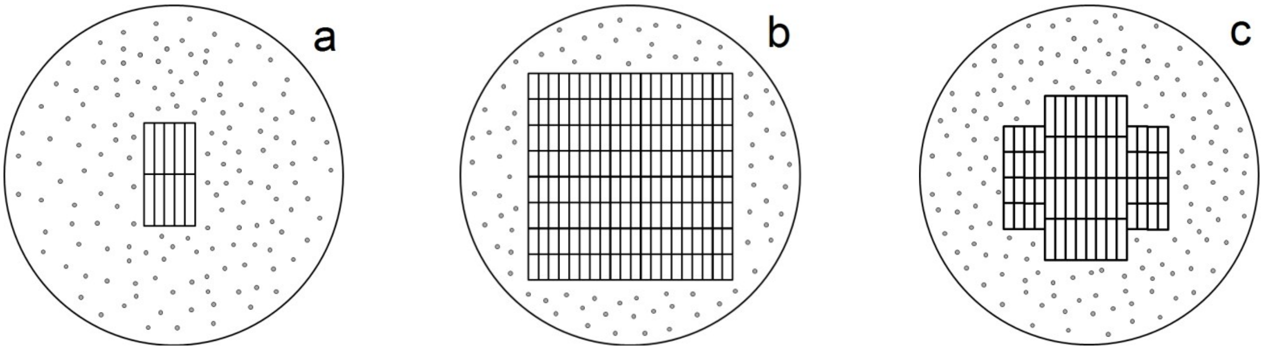

Figure 5. Models of the structures of nanoparticles of the η-phase (*a*), anatase (*b*), and the defect structure of the η-phase (*c*)

Therefore, based on the X-ray powder diffraction data and the results of the DD method, we propose a model of the three-dimensional structures of the main phases comprising sample I (Fig. 5*a*).

The limited possibilities of X-ray powder diffraction and DD methods for the determination of the nature and amount of water in sample I, which is also of importance for an understanding of the nature of phases, were supplemented by the results of conventional thermal analysis using polythermal heating (Fig. 6) and the storage under isothermal conditions for one hour in air at different temperatures.

As can be seen in the DTA-TGA curves (Fig. 6), the transformations of sample I are associated with continuous changes in its weigh in two temperature ranges (50-350°C and 500-650°C) and the decomposition processes that appear as endothermic peaks; the maximum rate of these processes are characterized by the peaks at ~90°C and 615°C.

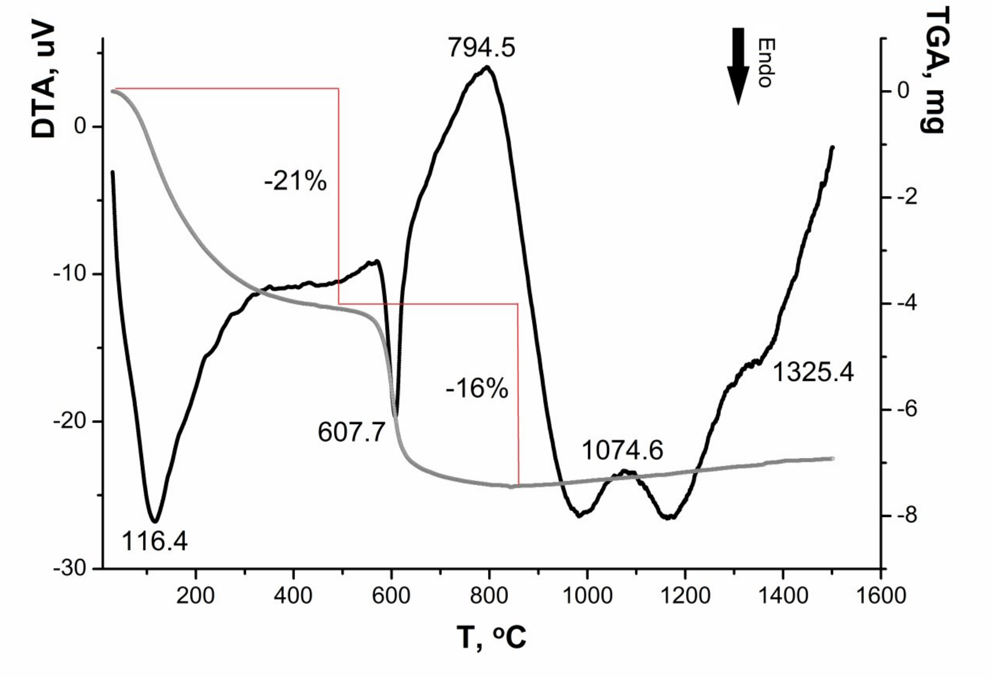

Figure 6. DTA-TGA curves for sample I in air

Based on the literature data [28-31], the weight loss in the range of 50-350°C is associated with the dehydration of the sample: adsorbed water molecules are removed at ~ 120ºC [32] and ~200°C [33, 34], and water molecules of crystallization and constitutional water are eliminated at ~250ºC and ~330ºC, respectively [32]. In the range of 500-650°C, chemisorbed OH groups and the sulfate component are lost, which is accompanied by the weight loss of ~21 and ~16 wt.%, respectively (in [35] the temperatures ~600-700°C were reported). Similar data on the total weight loss (~40 wt.%) and the presence of sulfate ions in samples at < 500ºC were reported in [34]. Three small exothermic peaks at 794°C, 1070°C, and 1330°C, which are almost not accompanied by the weight loss, are apparently attributed to the transition of nanocrystalline anatase to polycrystalline anatase and then to rutile [36, 37].

Therefore, the DTA-TGA curves confirm the presence of sulfate ions and OH groups in sample I determined by the DD method and are also indicative of the presence of water in this sample.

The absorption bands at 3320-3400 cm^{-1} are assigned to OH stretching vibrations of water molecules hydrogen-bonded to TiO_2, and the bands at 3200-3300 cm^{-1} belong to stretching vibrations of adsorbed water molecules (Table 2, fig. 7).

As the annealing temperature of sample I is increased, the amount of water molecules decreases, resulting in a decrease in the intensity and/or the disappearance of the corresponding vibrations in the IR spectra. Bending vibrations of water molecules appear as bands at 1619-1630 cm^{-1} (fig. 7). In the region of 1200 – 1055 cm^{-1} there are stretching and bending vibrations involving sulfate ions chemically bonded to titanium ions. An increase in the annealing temperature to 600–650^{o}C leads to a decrease in the intensity of these bands down to their complete disappearance, which is indicative of the removal of sulfate ions from the sample. In the region of 460–760 cm^{-1} bending vibrations of Ti…OH groups and stretching vibrations of TiO_6 octahedra (at frequencies lower than 600 cm^{-1}) are observed.

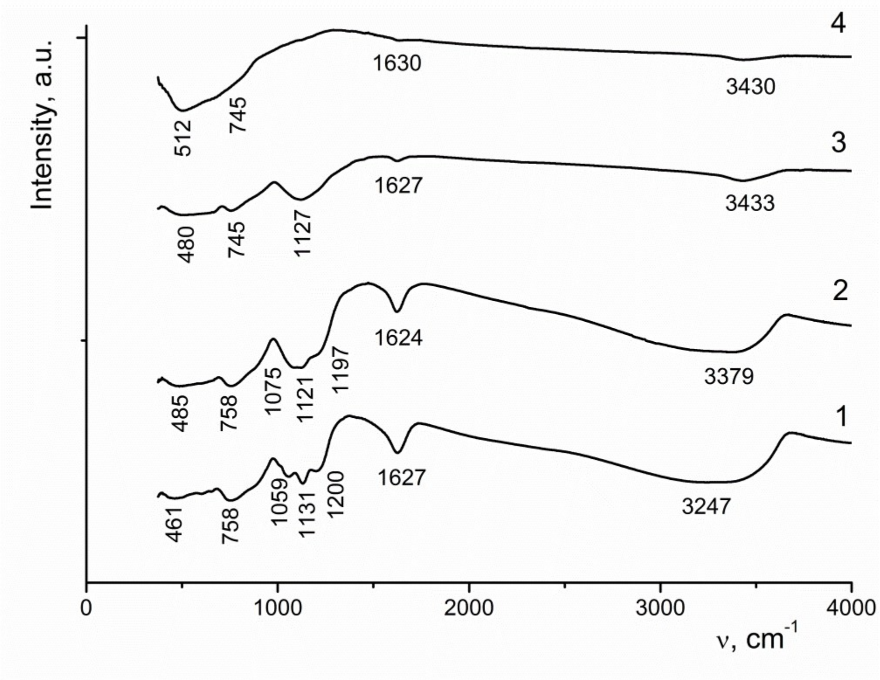

Figure 7. IR spectra of the initial sample I (1), I-200 (2), I-300 (3) and I-650 (4).

Table 2. Assignment of the bands in the IR spectra of the samples (based on the results published in [28, 29, 34, 38-40])

Assignment	Sample / wavenumber, cm^{-1}									
	I	**I-150**			**I-200**		**I-300**		**I-600**	**I-650**
	KBr	KBr	Nm	fo	Nm	fo	Nm	fo	KBr	Nm
ν(OH), (H_2O…Ti)		3348	3338	3326	3379		3433		3400- 3200	3430
ν(OH) (adsorbed H_2O)	3247	3271	3187		3296					
δ(HOH)	1627	1625	1625	1623	1624	1619	1627	1622	1600	1630
ν(S-O)	1200	1193	1188		1197					
δ(SO_4^{2-}), δ(TiOH)										1144*ben*
	1131	1128	1123		1121*sh*		1123*s*		1127*w*	
		1075	1075			1089*sh*				
	1059									
δ(TiOH)	758	758	759							
					745		745			
δ(TiOH), ν(TiO)										660
	602	597*m*	600*w*							
							512*br*		498	500*br*
		485*br*	484		480*br*					
	461									

Abbreviations: *br*, broad; *ben*, bending; *w*, weak; *sh*, shoulder; *s*, strong; *m*, medium, Nm, Nujol mulls; fo, fluorinated oil.

In order to get better understanding of the structures of the phases, we used Raman spectroscopy, which identifies these phases based on the local symmetry of chemical bonds. The Raman spectrum of sample I showing peaks at ~156cm^{-1} (E_g), 415 cm^{-1}(B_{1g}), ~ 506 cm^{-1} (A_{1g} B_{1g}), and 625 cm^{-1} (E_g) provides evidence that the local bond order is similar to that in the anatase structure (Fig. 8).

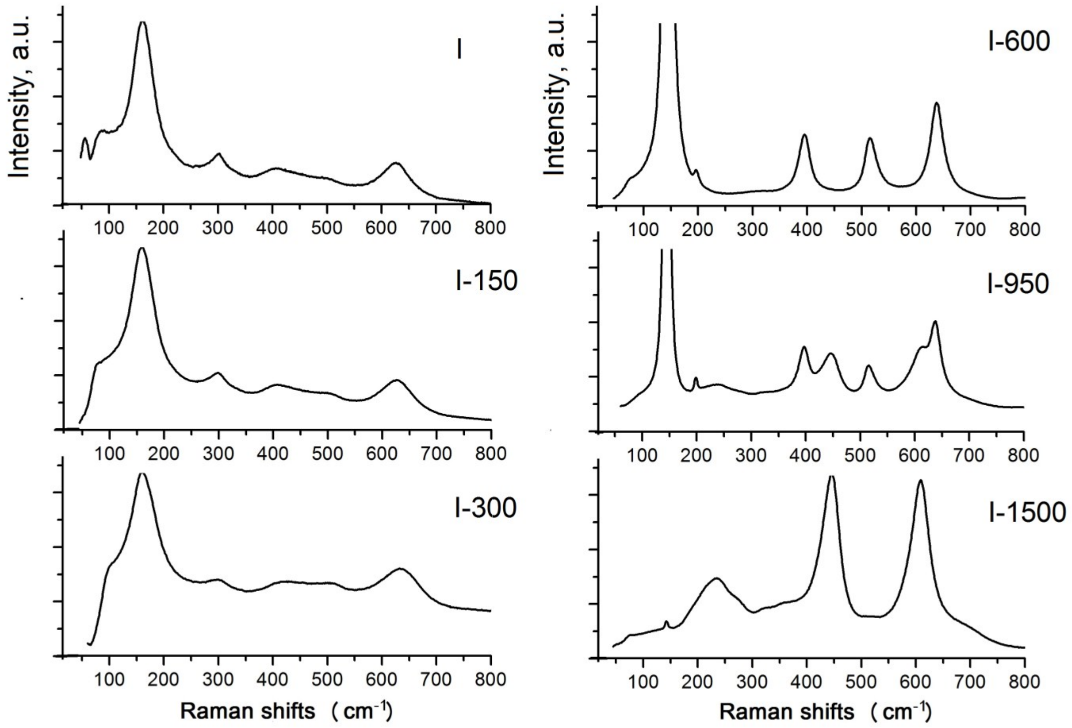

Figure 8. Raman spectra of the starting sample I and the samples annealed at different temperatures

However, judging from the diffuse character and low intensities of the bands (particularly, the peak at 506 cm^{-}1), particles of the phases are amorphous and nanocrystalline. The broadened and asymmetric shape of the peak at 156 cm^{-1} results from the amorphous state of the phase B1, which is usually attributed to the disorder in Ti-O distances of TiO_6 octahedra due to low dimensionality of the particles and the reconstruction of their surface *via* the sulfurization and hydrations [30, 34, 41, 42]. The diffuse character of the lines in the regions of 400-425 and 624-640 cm^{-1} is attributed to the presence of nanocrystallites of B2. In the absence of the peak at 226 cm^{-1} characteristic of the hydrated form of titanium dioxide, the B2 phase can be assigned with confidence to dioxide nature, in particular, to the η- phase [22, 23]. In [30] the bands at 430 and 605 cm^{-1} are considered as a sign of the amorphous state of the product.

The character of the Raman spectrum of sample I-150 is almost identical to that of the initial sample. A weak tendency of the band at 156 cm^{-1} to be shifted to lower frequencies and the shift of the bands at 430 and 605 cm^{-1} to higher frequencies are due to a decrease in the disorder in the Ti-O distances. The band at 300 cm^{-1} that disappears after the annealing is apparently assigned to Ti-OH vibrations.

The set of peaks in the Raman spectrum of sample I-600 corresponds to anatase. A further increase in the annealing temperature leads to the polymorphic transformation of anatase to rutile accompanied by the appearance of vibrational modes at 440 and 610 cm^{-1} characteristic of rutile. The bands at 85 cm^{-1} and at lower frequencies apparently correspond to boson vibrations associated with elastic vibrations in inhomogeneities of the structure or with certain weak, probably interionic, interactions between oxygen-containing groups in the titanium oxygen network.

The results of investigation of sample I by a complex of methods prove that this sample is not single-phase, and the surface of low-dimensional amorphous nanoparticles of two of the three identified phases was non-uniformly coated with hydroxyl and sulfate groups. The fact that the sample is not single-phase is attributed to the incomplete hydrolysis and fast coagulation, resulting in the precipitation of all chemical forms of titanium of different degrees of polymerization that are present at the moment of precipitation.

The overall composition of the η-phase based on the results of investigations by all methods can be written as $[TiO_{2-x}\cdot mH_2O](OH)_y(HSO_4)_z\cdot nH_2O$. In [9] it was noted that the η-phase contains sulfur, which exists apparently in the form of SO_4. After washing with water followed by the neutralization, sulfate groups are replaced by hydroxyl groups without degradation of the phase $[TiO_{2-x}\cdot mH_2O](OH)_y\cdot nH_2O$, *i.e.*, the η-phase has a variable composition. In fact, a similar composition is assigned to hydrated titanium(IV) oxide $Ti^{4+}O_{2-y/2}(OH)_y\cdot nH_2O$ [9], as well as to $(TiO_{1.9})(OH)_{0.2}\cdot nH_2O$ with a distorted anatase structure [43], in which OH groups can be partially replaced by sulfate groups (phase A) [9] when employing the sulfate method for the preparation of samples (Table 1, Fig. 4).

A sample with the η-phase can be prepared not only by the hydrolysis of titanyl sulfate $TiOSO_4\cdot xH_2SO_4\cdot yH_2O$ but also by the hydrolysis of an aqueous solution of $TiOSO_4\cdot 2H_2O$ in the presence of such strong acids as $HClO_4$, HNO_3 [44], and H_2SO_4. It should be noted that in the absence of acids or in the presence of the weak acid CH_3COOH, the reaction affords anatase, whereas in the presence of the weak acid H_3PO_4

titanium dioxide is not formed [44]. These experimental data indicate that the regions of the existence of the η-phase and nano-anatase are controlled by the pH value of the reaction system.

The η-phase – nano-anatase phase transitions can be visualized based on the disappearance of the diffraction reflection at 2θ = ~4.3–5.3º and the splitting of the diffraction reflection at 2θ~38°: amorphous TiO_2 (*D*<~30 Å), nano-η-TiO_2 (*D*~30–50 Å; 2θ~5°, ~25°, ~33°, ~38º), nano-anatase (I) (*D*~50–100 Å; 2θ~38°), and nano-anatase (II) (*D*~100–500 Å; 2θ~37°, ~38°, ~39°) (Fig. 9).

Therefore, as can be seen in Figs 2*a* (3) and 5 and according to the results of the study [32], adsorbed water molecules are responsible for a small-angle peak characteristic of the η-phase, which is absent in the diffraction pattern of sample I-150. It is the reflection with *d*~17–21Å in the diffraction patterns of the samples with the η-phase that changes in the angle range 2θ=~4.3–5.3º with a change in the intensity [9, 20], whereas the other diffraction peaks characteristic of the η-phase are stable to a certain extent. Hence, it can be concluded that the structure of the η-phase is stabilized by water molecules located between the layers, thus facilitating the formation of a quasi-layered structure with the large unit-cell parameter *c*, the crystallites being platelet-like [20] (Fig. 5*a*). In other words, the structure of the η-phase can be considered as an intercalate. Thus, the structure consists of layers of TiO_6 octahedra (probably, TiO_5 as well) with an anatase-like structure and water molecules, which are located between the layers and are hydrogen-bonded to oxygen atoms. These data suggest that the η-phase is a pseudopolymorph, *viz*., titanium dioxide solvate (hydrate), rather than a polymorph of TiO_2.

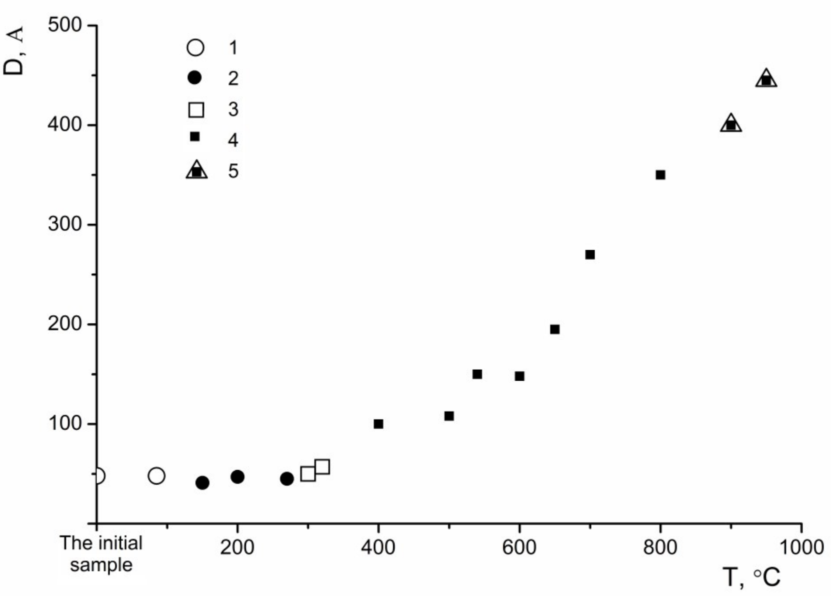

Figure 9. Dependence of the average sizes of coherent scattering regions (D, A) on the annealing temperature of the sample with the η-phase: 1 – η-phase; 2 – η-phase + nano-anatase (I); 3 – nano-anatase (I); 4 – nano-anatase (II); 5 – nano-anatase (II) + nano-rutile.

Nevertheless, the formation of low-dimensional titanium(IV) oxides, the overall compositions of which can be described as $[TiO_{2-x}(OH)_x](OH)_y(HSO_4)_z\cdot nH_2O$ and $[TiO_{2-x}\cdot mH_2O](OH)_y(HSO_4)_z\cdot nH_2O$ with $z \geq 0$, cannot be ruled out as well. The structures of these phases are determined by the regular structure of $[TiO_{2-x}(OH)_x]$ (nano-anatase with x=0 and distorted nano-anatase, apparently, with x>0) and $[TiO_{2-x}\cdot mH_2O]$ (η-modification) containing different amounts of adsorbed interlayer water (characterized by the peak at *d* ~ 17–21 Å and a variation in the unit cell parameter *c*), as well as by the specificity of the structure that differs from anatase (which is probably characterized by the reflection at 2θ~33° with *d*~2.7 Å). These phases are composed of a disordered amorphous layer with titanium(IV) oxide modified by sulfate and/or hydroxyl groups and adsorbed water. The ratio of these constituents (the core and the shell, respectively) determines primarily the average size of coherent scattering regions (crystallites) (Fig. 5), whereas the composition of the shell is responsible mainly for the specific surface area and, consequently, photocatalytic, sorption, bactericidal, *etc*. properties.

Conclusion

Samples with the η-phase were prepared by the hydrolysis of titanyl sulfate $TiOSO_4\cdot xH_2SO_4\cdot yH_2O$. The stability region of this phase in the hydrolysis temperature–hydrolysis duration coordinates was determined. It is shown that nanoparticles of the η-phase consist from a core and a shell. The core has $[TiO_{2-x}\cdot mH_2O]$ composition, the structure of which can be described as a superstructure in relation to anatase structure. The structure of the η-phase can be considered as an intercalate with the water molecules located between the layers of TiO_6 octahedrons. The cell parameter *c* depends on the content of water: it increases (decreases) with increase (reduction) molecules of water in interlayered space.

The amorphous shell of η-phase contains TiO_{2-x} (trace amount), OH, HSO_4 and water. According to composition, this phase is not a polymorph of TiO_2 and is a pseudo-polymorph of titanium dioxide hydrate. The average crystallite size depends on the ratio of a core thickness and shell one of nanoparticles. At temperature increase (to ~250°C) the phase η-phase passes into a phase with anatase structure with water loss. It is followed by increase in the sizes of crystallites.

Acknowledgements

The present study was financially supported by RFBR (research project No. 13-03-00367).

Notes and references

1 Andrievskiy R A and Glezer A M 1999 *Phys. of Metals and Metallography* 88 (1) 50-73

2 Gnaser H, Huber B and Ziegler C In *Encyclopedia of Nanoscience and Nanotechnology*; Nalwa HS, Ed.; American Scientific Publishers: Stevenson Ranch 2004 6 505-535

3 Chen H J, Jian P C, Chen J H, Leeyih W and Chiu W Y 2007 *Ceram. Int.* 33 643

4 Kokila V, Senthilkumar K and Nazeer P 2011 *Archives of Physics Research* 2 (1) 246-253

5 Ohtani B 2013 *Catalysts* 3 942-953

6 Fujishima A, Hashimoto K and Watanabe T TiO_2 *Photocatalysis: fundamentals and applications*; BKC: Tokio, 1999 242

7 Reddy P A K, Reddy P V L, Sharma V M, Srinivas B, Kumari V D and Subrahmanyam, M 2010 *J. Water Resource and Protection* 2 235-244

8 Buzby S, Barakat M A, Lin H, Ni C, Rykov S A, Chen J G, Ismat Shah S 2006 *J. Vac. Sci. Technol. B* 24 (3), 1210-1214

9 Dadachov M. U.S. Patent Application Publication 2006/0171877

10 Dadachov M. U.S. Patent Application Publication 2006/0144793

11 Savinkina E V, Obolenskaya L N, Kuz'micheva G M, Dorokhov A V and Tsivadze A U 2011 *Doklady Physical Chemistry* 441 (1) 224-226 DOI: 10.1134/S0012501611110042. http://link.springer.com/article/10.1134%2FS0012501611110042

12 Kuz'micheva G M, Savinkina E V, Titov D N, Demina P A, Obolenskaya L N, Bruk L G, Yakovenko A G and Chernobrovkin M G 2011 *Inorganic Materials* 47 (7) 753-758 DOI: 10.1134/S002016851106015X, http://link.springer.com/article/10.1134%2FS002016851106015X

13 Savinkina E V, Kuz'micheva G M, Obolenskaya L N and Domoroshchina E N Rus. Patent 2469954.

14 Warren B E 1990 *X-Ray Diffraction*; Dower Publications: New York 381.

15 Kuz'micheva G M, Gainanova A A and Podbel'skiy V V Rus. Patent 2014660201

16 Malakhov V V and Vasil'eva I G 2008 *Russian Chemical Reviews* 77 (4) 351-372 DOI: 10.1070/RC2008v077n04ABEH003737.

17 Jerman Z 1966 *Collection Czechoslov. Chem. Commun*. 31, 3280-3286.

18 Bekkerman L I, Dobrovol'skiy I P and Ivkin A A 1976 *Russian journal of inorganic chemistry* 31, 418

19 Pervushin V U, Tolchev A V, Denisova T A and German V A 1989 *Russian journal of inorganic chemistry* 34, 1096.

20 Kuz'micheva G M, Gainanova A A, Orekhov A S, Klechkovskaya V V, Sadovskaya N V and Chernyshov V V 2014 *Crystallography Reports* 59 (6) 1008-1014 DOI: 10.1134/S1063774514050101 http://link.springer.com/article/10.1134/S1063774514050101

21 Obolenskaya L N, Zaporozhets M A, Kuz'micheva G M and Savinkina E V 2015 *Crystallography Reports* 60 (3) 455

22 Kuz'micheva G M, Savinkina E V and Obolenskaya L N 2010 *Crystallography Reports* 55 (5) 866-871 DOI: 10.1134/S1063774510050287, http://link.springer.com/article/10.1134%2FS1063774510050287

23 Kuz'micheva G M, Savinkina E V, Belogorokhova L I, Mavrin B N and Flid V R 2011 *Russian Journal of Physical Chemistry A* 85 (6) 1037-1040 DOI: 10.1134/S0036024411060203, http://link.springer.com/article/10.1134%2FS0036024411060203

24 Hino M and Arata K 1988 *J. Chem. Soc. Chem. Comm* 18 1259-1260

25 Lungren G 1959 *Svensk. Kem. Tidskrift.* 71 200-220

26 Ganchenko L G, Kiselev V F and Murina V V 1961 *Russian Journal of Kinetics and Catalysis* 11 877.

27 Cheng H, Ma J, Zhao Z and Qi L 1995 *Chem. Mater.* 7 663-671

28 Li G, Li L, Boerio-Goates J and Woodfield B 2005 *J. Amer. Chem. Soc.* 127 8659

29 Yang Q, Xie C, Xu Z, Gao Z and Du Y 2005 *J. Phys. Chem. B* 109 5554-5560

30 Zhang J, Li M, Feng Z, Chen J and Li C 2006 *J. Phys. Chem. B* 110 927-935

31 Ivicheva S N, Kargin U F, Kutsev S V, Shvornena L I and Urkov G U 2013 *Physics of the solid states* 55 (5) 1111-1119 DOI: 10.1134/S1063783413050132, http://link.springer.com/article/10.1134%2FS1063783413050132

32 Kostrikin A V, Kuznetsova R V, Kosenkova O V, Merkulova A N and Lin'ko I V 2007 *Problems of contemporary science and practice (Russian journal)* 2 (8) 181-186

33 Kanna M, Wongnawa S, Sherdshoopongse P and Boonsin P 2005 *J. Sci. Technol.* 27 (5) 1017-1026

34 Esteban Benito H, Del Angel Sancher T and Galeria Alamilla R 2014 *Brazilian J. of. Chem.* 31 (3) 737-745

35 Serikov A S, Gladkov V E, Zherebtsov D A, Kolmogortsev A M and Viktorov V V 2010 *Bulletin of the South Ural state University (Chemistry)* 4 (31) 97-101

36 Riyas S, Krishnan G A and Mohan Das P N 2006 *Journal of Ceramic Processing Research* 7 (4) 301-306

37 Ha P S, Youn H-J, Jung H S, Hong K S, Park Y H and Ko K H 2000 *J. Colloid Interf. Sci.* 223 16-20

38 Qian L, Du Z L, Yang S Y and Jin Z S 2005 *J. Mol. Struct.* 749 103-107.

39 Yan M, Chen F, Zhang J and Anpo M 2005 *J. Phys. Chem. B* 119 8673-8678

40 Bezrodna T, Puchkovska T, Shymanovska V, Baran J and Patajczak H 2004 *J. Molec. Struct.* 700 175-181

41 Kelly S, Pollak F H and Tomkiewicz M 1997 *J. Phys. Chem.* B 101 2730

42 Dimitrijevic N M, Saponjic Z V and Rabatic B M 2007 *J. Phys. Chem. Lett.* 111 7235-7241

43 Denisova T A Ph.D. Thesis. Institute of Chemistry, Ural Branch of the Russian Academy of Sciences. Ekaterinburg, Russia, 1985.

44 Kuz'micheva G M and Gainanova A A Rus. Patent Application Publication No. 2014137971

New Journal of Chemistry

ARTICLE

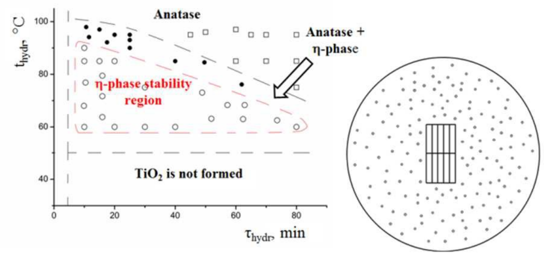

The low-temperature η-phase consist of the $[TiO_{2-x}\cdot mH_2O]$ core and an amorphous shell containing TiO_{2-x} (trace), OH, HSO_4 and water